Synthesis, Molecular Modeling Studies, and Preliminary Pharmacological Characterization of All Possible 2-(2′-Sulfonocyclopropyl)glycine Stereoisomers as Conformationally Constrained *L*-Homocysteic Acid Analogs

Roberto Pellicciari,*[,†] Maura Marinozzi,[†] Antonio Macchiarulo,[†] Maria Carmela Fulco,[†] Julia Gafarova,[†,§] Michaela Serpi,[†] Gianluca Giorgi,[‡] Søren Nielsen,[||] and Christian Thomsen[||]

Dipartimento di Chimica e Tecnologia del Farmaco, Università di Perugia, Via del Liceo, 1- 06123 Perugia, Italy, Dipartimento di Chimica, Università di Siena, Via A. Moro, 53100 Siena, Italy, and H. Lundbeck A/S, 9 Ottilavej, DK-2500 Valby, Copenhagen, Denmark

Received March 21, 2007

Bioisosteric replacements of the distal acidic group of *L*-glutamic acid (*L*-Glu, **1**) and conformational constraining of its carbon skeleton, have been widely exploited to discover competitive modulators of glutamate receptors. Noteworthy, *L*-homocysteic acid (*L*-HCA, **18**), a neurotransmitter belonging to the class of excitatory sulfur-containing amino acids, may be considered an endogenous occurring bioisoster of *L*-Glu (**1**). *L*-HCA (**18**) has been reported to mediate signaling between glial cells and postsynaptic neurons through the activation of glutamate receptors and others hitherto not well-characterized receptors. As a continuation of our work in the preparation of conformationally constrained glutamate analogs, we report the synthesis and the preliminary pharmacological characterization at iGluRs and mGluRs of all eight stereoisomers of 2-(2′-sulfonocyclopropyl)glycine (SCGs, **8**−**15**). Among the reported compounds, *S*-SCG-4 (**15**) showed to be a potent and relatively selective AMPA ligand. Docking experiments coupled to molecular electrostatic potential calculations allowed insight into the molecular basis of the activity of this compound to be gained. The library of SCGs (**8**−**15**), while providing a novel source of modulators of the glutamate receptors, represents a valuable chemical tool to better characterize *L*-HCA pathways in the CNS.

Introduction

The medicinal chemistry of *L*-glutamic acid (*L*-Glu,[a] **1**), the main excitatory neurotransmitter in the mammal central nervous system (CNS), has historically relied on two main strategies to discover selective and potent competitive modulators of glutamatergic receptors: (i) the conformational freezing of the carbon skeleton through different ring insertions and (ii) the bioisosteric replacement of the distal carboxylic group. The exploitation of these strategies, used in single or combined approaches, yielded several classes of glutamate analogs. For instance, (carboxycyclopropyl)glycine derivatives (CCGs, **2**−**5**) have represented in the past a valuable source of potent and selective ligands for the various members of both ionotropic- and metabotropic glutamate receptor families (iGluRs and mGluRs).[1−6]

Pursuing a combined approach, we recently described the design and synthesis of 2-(2′-phosphonocyclopropyl)glycines (*S*-PCG-1, **6**, and *S*-PCG-2, **7**) as selective modulators of group III mGlu receptors.[7]

In a framework aimed at complementing our recent studies[8] on the bioisosterism of acidic groups and as a continuation of our work in the preparation of cyclopropyl-constrained *L*-Glu analogs, herein we report the synthesis and the preliminary pharmacological characterization of all eight stereoisomers of 2-(2′-sulfonocyclopropyl)glycine (SCGs, **8**−**15**).

It is worth noting that these compounds may be well considered as cyclopropyl-constrained analogs of *L*-homocysteic acid (*L*-HCA, **18**), an endogenous occurring bioisoster of *L*-Glu (**1**). *L*-HCA is a neurotransmitter belonging to the class of excitatory sulfur-containing amino acids (ESAAs, Chart 3), which originate from the degradation pathway of *L*-homocysteine, and additionally comprise *L*-cysteic acid (*L*-CA, **16**), *L*-cysteine sulfinic acid (*L*-CSA, **17**), and *L*-homocysteine sulfinic acid (*L*-HCSA, **19**).[9]

In particular, *L*-HCA (**18**) is a potent neuronal excitant activating iGluRs and to a lesser extend mGluRs (Table 1). *L*-HCA (**18**) is almost exclusively localized in glial cells of various brain regions[10−13] where it is released upon activation of both glial β-adrenergic receptors and glutamate receptors.[14,15] These findings, coupled to the notion that glial cells are actively involved in CNS development and function,[16,17] indicate that **18** may cover a pivotal role as gliotransmitter in modulating the synaptic transmission.[18]

Interestingly, an excessive activation of central excitatory receptors by high concentrations of *L*-HCA (**18**) has been proposed as the pathogenic mechanism linking the effect of elevated blood concentrations of homocysteine[19] to a number of neuronal disorders such as Alzheimer's disease, schizophrenia, cognitive dysfunctions, and neural tube defects,[20−24] as

* To whom correspondence should be addressed. Tel: +39 075 5855120. Fax: +39 075 585 5124. E-mail: rp@unipg.it.
[†] Università di Perugia.
[‡] Università di Siena.
[§] On leave from Institute of Organic Chemistry, Ufa Research Center, Russian Academy of Sciences, Ufa, Russia.
[||] H. Lundbeck A/S.

[a] Abbreviations: AC, adenyl-cyclase; AMPA, α-amino-3-hydroxy-5-methylisoxazole-4-propionic acid; CCG, 2-(2′-carboxycyclopropyl)-glycine; CNS, central nervous system; DAMS, *neo*pentyl diazomethanesulfonate; ESAA, excitatory sulfur-containing amino acid; iGluR, ionotropic glutamate receptor; *L*-AP4, *L*-4-aminophosphonic acid; *L*-CA, *L*-cysteic acid; *L*-CSA, *L*-cysteine sulfinic acid; *L*-Glu, *L*-glutamic acid; *L*-HCA, *L*-homocysteic acid; *L*-HCSA, *L*-homocysteine sulfinic acid; LiHMDS, lithium bis(trimethylsilyl)amide; mGluR, metabotropic glutamate receptor; MPC, medium pressure chromatography; PCA, principal component analysis; PCC, pyridinium chlorochromate; PCG, 2-(2′-phosphonocyclopropyl)glycine; PLD, phospholipase D; SCG, 2-(2′-sulfonocyclopropyl)glycine; TMSCN, trimethylsilyl cyanide.

10.1021/jm070322e CCC: $37.00
Published on Web 08/29/2007

Chart 1. 2-(2′-Carboxycyclopropyl)glycines as Conformationally Constrained *L*-Glu Analogs

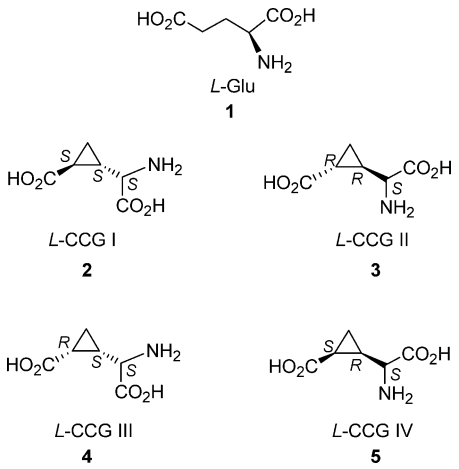

Chart 2. 2-(2′-Phosphonocyclopropyl)glycines as Conformationally Constrained Bioisosteric Analogs of *L*-Glu

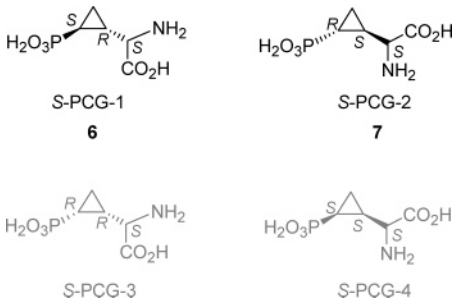

Chart 3. Excitatory Sulfur-Containing Amino Acids (ESAAs)

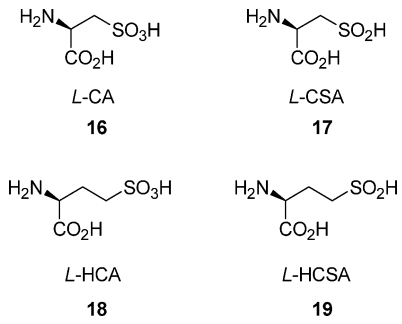

observed in patients with severe and moderate forms of hyperhomocysteinemia.

Despite the increasing interest in the physiological and pathological roles of ESAAs and particularly of *L*-HCA (**18**) in the brain, a thorough characterization of their pathways is still elusive.

In this scenario, SCGs (**8**−**15**), while providing a novel source of modulators of the glutamate pathways, represent valuable chemical tools to study the physiological and pathological roles of *L*-HCA (**18**) in the brain.

Chemisty

The synthesis of the complete stereolibrary of *cis*- and *trans*-SCGs (**8**−**15**), the aim of the present work, proved to be a challenging task. A survey of the literature at the beginning of our work revealed the availability of very few routes for the preparation of sulfonyl-substituted cyclopropane derivatives and all the routes leading selectively to the synthesis of *trans*-stereoisomers. It had been reported, in particular, that *trans*-aryl- and alkyl-cyclopropyl sulfones could be prepared by α,γ-dehydrohalogenation of γ-chlorosulfones,[25] a route also utilized for the synthesis of *trans*-2-aryl cyclopropylsulfonic acid esters and amides.[26] The latter derivatives were also prepared by the addition of dimethylsulfonium methylide to the corresponding *trans*-2-arylethenesulfonic acid derivatives.[27] 2-(2′-Phenylsulfonocyclopropyl)glycines, as a mixture of the four *trans*-stereoisomers, have previously been prepared by Michael addition of a glycine equivalent to 3-bromoprop-1-enyl phenyl sulfone.[28] An alternative, more versatile route for the preparation of 2-substituted cyclopropylsulfonic acid derivatives could involve the catalyzed decomposition of an α-diazosulfonyl esters in the presence of a suitable olefin. It should be pointed out, at this regard, that in contrast with the widely studied and synthetically exploited α-diazocarbonyl compounds, the analogous diazosulfonyl compounds, namely, α-diazosulfones and α-diazosulfonates, have received comparatively very little attention.[29−35] α-Diazoalkanesulfonates, chosen as key reagents for the preparation of our title compounds, were almost unknown at the beginning of our work. Indeed, only one paper reported their preparation in low yields by submitting to deformylating diazo group transfer reaction the corresponding formylalkanesulfonates.[36] Recently, the first example of copper- and rhodium-catalyzed cyclopropanation of a series of simple alkenes with α-diazoalkanesulfonates appeared in the literature.[37] The authors prepared DAMS (**20**) by a detrifluoroacetylating diazo group transfer reaction in good yield (60%).

The reaction of DAMS (**20**) with 1,3-pentadiene (**21**) was then carried out using copper(I) triflate as the catalyst (Scheme 1). Compound **21** reacted exclusively at the less-substituted double bond affording the mixture of the corresponding *E*,*E*-, *E*,*Z*-, *Z*,*E*-, and *Z*,*Z*-*neo*pentyl 2-(prop-1-enyl]cyclopropanesulfonates (**22**−**25**) in 1.0:1.7:2.6:1.2 ratio, respectively (GC).

Flash chromatography provided the mixtures of *E*,*E*- and *E*,*Z*-isomers (±)-**22** + (±)-**23** and *Z*,*E*- and *Z*,*Z*-isomers (±)-**24** + (±)-**25** in 42% and 32% yields, respectively. Ozonolysis of the propenyl side chain of the mixture (±)-**22** + (±)-**23**, carried out at − 78 °C in dichloromethane, followed by quenching with methyl sulfide, afforded the corresponding *trans*-aldehyde (±)-**26** in 66% yield. Analogously, starting from the *Z*,*E*- and *Z*,*Z*-isomer mixture (±)-**24** + (±)-**25**, the corresponding *cis*-aldehyde (±)-**27** was obtained in 72% yield. The relative configurations of the aldehydes (±)-**26** and (±)-**27** were established by spectroscopic analysis. In particular, chemical shift values of the proton geminal to the aldehydic group, which is more deshielded in the diastereoisomer (±)-**26** (2.8 ppm as against 2.2 ppm for (±)-**27**) due to the proximity with the sulfonate moiety, were clarifying. In a stereoselective way, the *trans*-aldehyde (±)-**26** could be alternatively prepared by an intramolecular epoxide opening reaction promoted by a carbanion generated at the α-position of the sulfonyl moiety (Scheme 2). To this end, *neo*pentyl 2-oxiran-2-ylethanesulfonate (**30**) was prepared starting from 4-bromobutene (**28**) using standard procedures[38] and then submitted to the intramolecular epoxide opening reaction promoted by lithium bis(trimethylsilyl)amide. By this way, *trans*-neopentyl 2-(hydroxymethyl)cyclopropyl sulfonate [(±)-**31**] was exclusively obtained in 65% yield, which, by subsequent oxidation with PCC, gave the desired *trans*-aldehyde (±)-**26**.

With the two racemic aldehydes (±)-**26** and (±)-**27** in our hand, the transformation of each of them into the corresponding four possible enantiopure SCGs was addressed, by a diastereoselective Strecker reaction involving (*R*)-α-phenylglycinol as the chiral auxiliary.[39] The *trans*-aldehyde (±)-**26** was then submitted to condensation with *R*-α-phenylglycinol (Scheme 3),

Table 1. Glutamate Receptor Inhibitory Constants of 2-(2′-Sulfonocyclopropyl)glycines (**8**−**15**)[a]

cmpd	mGluR1 K_i (μM)	mGluR5 K_i (μM)	mGluR2 K_i (μM)	mGluR4 K_i (μM)	NMDA K_i (μM)	KA K_i (μM)	AMPA K_i (μM)
S-SCG-1 (**8**)	34 ± 9	49 ± 2	235 ± 29	>300	>300	>300	>300
S-SCG-2 (**9**)	77 ± 8	81 ± 5	>300	>300	>300	34 ± 8	>300
R-SCG-1 (**10**)	254 ± 34	67 ± 10	>300	>300	150 ± 23	71 ± 8	72 ± 12
R-SCG-2 (**11**)	>300	>300	>300	>300	22 ± 5	34 ± 7	96 ± 13
S-SCG-3 (**13**)	>300	>300	>300	>300	>300	>300	>300
R-SCG-3 (**12**)	>300	>300	>300	>300	>300	35 ± 9	>300
S-SCG-4 (**15**)	>300	>300	>300	>300	19 ± 7	3.3 ± 0.4	0.10 ± 0.007
R-SCG-4 (**14**)	>300	55 ± 19	>300	>300	61 ± 9	64 ± 14	72 ± 15
L-Glu (**1**)	0.25 ± 0.03	0.39 ± 0.06	11 ± 2	2.4 ± 0.5	0.20 ± 0.04	0.07 ± 0.02	0.08 ± 0.03
L-HCA (**18**)	87 ± 35	54 ± 17	>300	53 ± 8	2.7 ± 0.7	9.9 ± 1.1	2.4 ± 0.2

[a] Data are the mean ± SEM of 3−5 determinations performed in triplicate as described previously.[66−70] IC_{50} values were calculated from competition binding experiments by a nonlinear regression analysis and used for calculation of K_i values according to the following equation: $K_i = IC_{50}/(1 + [L]/K_d)$, where $[L]$ is the concentration of radioligand and K_d is its dissociation constant.

Scheme 1[a]

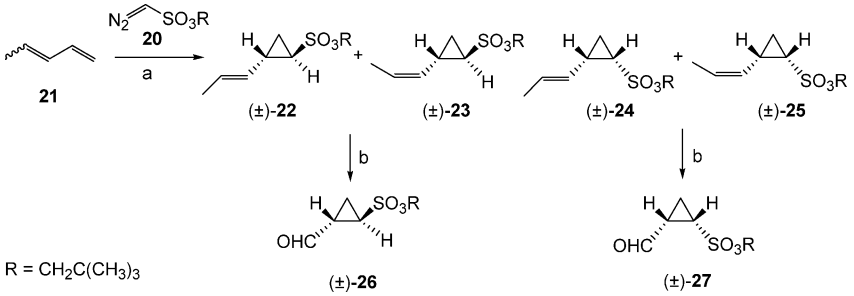

[a] Reagents and conditions: (a) $(CF_3SO_3Cu)_2 \cdot C_6H_6$, rt; (b) (i) O_3, CH_2Cl_2, −78 °C; (ii) Me_2S, −78 °C to rt.

Scheme 2[a]

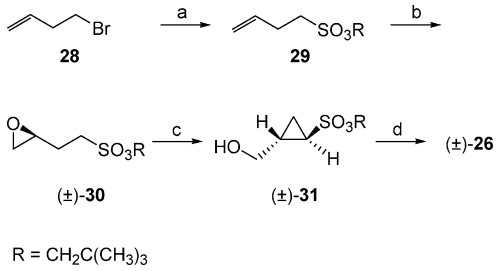

[a] Reagents and conditions: (a) ref 55; (b) *m*CPBA, CH_2Cl_2, rt; (c) LiHMDS, THF, −30 °C; (d) PCC, CH_2Cl_2, rt.

and the Schiff base thus formed, reacted with trimethylsilyl cyanide to afford a mixture of the four expected α-amino nitriles **32**−**35**, as two major and two minor components (34:38:12:16 by HPLC).[40]

Medium-pressure chromatography (MPC) of the reaction mixture allowed the separation of the desired four [(*R*)-(phenylglycinyl)amino]nitriles **32**−**35** in 15, 21, 7, and 6% yields, respectively. The derivative **32** was then submitted to oxidative cleavage of the chiral auxiliary, acidic hydrolysis, and purification by ion-exchange resin chromatography to afford (2*S*,1′*R*,2′*S*)-2-(2′-sulfonocyclopropyl)glycine (*S*-SCG-1, **8**) in 32% yield. By an analogous procedure, starting from the amino nitriles **33**−**35**, (2*S*,1′*S*,2′*R*)-2-(2′-sulfonocyclopropyl)glycine (*S*-SCG-2, **9**), (2*R*,1′*S*,2′*R*)-2-(2′-sulfonocyclopropyl)glycine (*R*-SCG-1, **10**), and (2*R*,1′*R*,2′*S*)-2-(2′-sulfonocyclopropyl)glycine (*R*-SCG-2, **11**) were obtained in 40, 45, and 45% yields, respectively.

The preparation of the four SCGs (**12**−**15**), endowed with a folded disposition between sulfonate and glycine moieties, was achieved in the same fashion by using *cis-neo*pentyl 2-formylcyclopropanesulfonate (±)-**27** as the starting material (Scheme 4).

The above-described synthetic protocol involving diastereoselective Strecker with *R*-α-phenylglycinol, oxidative cleavage

Scheme 3[a]

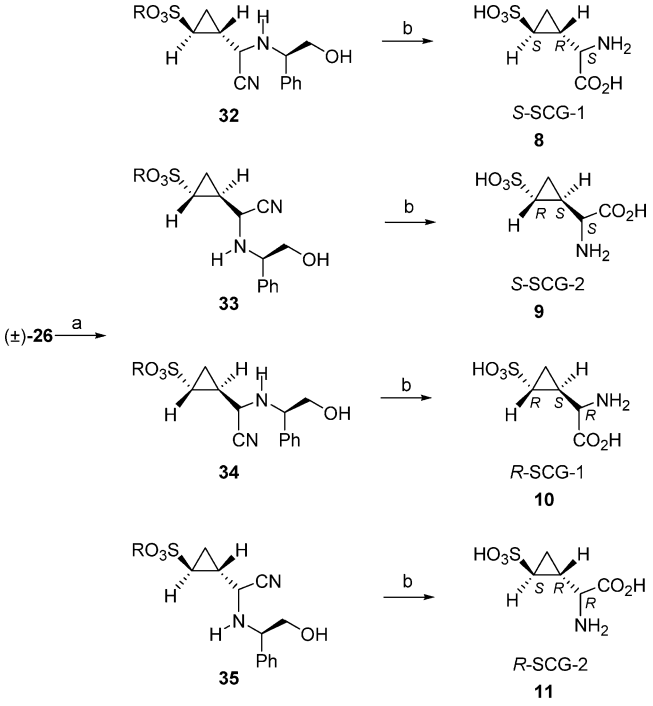

[a] Reagents and conditions: (a) (i) *R*-α-phenylglycinol, MeOH, rt; (ii) TMSCN, 0 °C to rt; (iii) MPC; (b) (i) $Pb(OAc)_4$, CH_2Cl_2−MeOH, 0 °C; (ii) 6 N HCl, 95 °C; (iii) Dowex 1 × 8 200, 1 N HCl.

followed by acidic hydrolysis, and purification by ion-exchange resin chromatography, provided (2*R*,1′*S*,2′*S*)-2-(2′-sulfonocyclopropyl)glycine (*R*-SCG-3, **12**), (2*S*,1′*R*,2′*R*)-2-(2′-sulfonocyclopropyl)glycine (*S*-SCG-3, **13**), (2*R*,1′*R*,2′*R*)-2-(2′-sulfonocyclopropyl)glycine (*R*-SCG-4, **14**), and (2*S*,1′*S*,2′*S*)-2-(2′-sulfonocyclopropyl)glycine (*S*-SCG-4, **15**) in 16, 17, 2, and 8% overall yields, respectively.

Scheme 4[a]

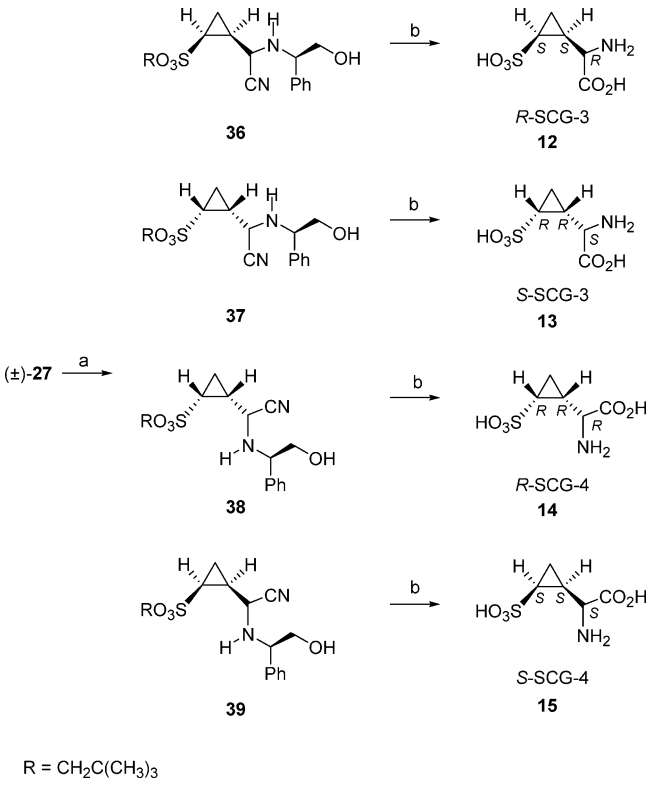

[a] Reagents and conditions: (a) (i) *R*-α-phenylglycinol, MeOH, rt; (ii) TMSCN, 0 °C to rt; (iii) MPC; (b) (i) $Pb(OAc)_4$, CH_2Cl_2−MeOH, 0 °C; (ii) 6 N HCl, 95 °C; (iii) Dowex 1 × 8 200, 1 N HCl.

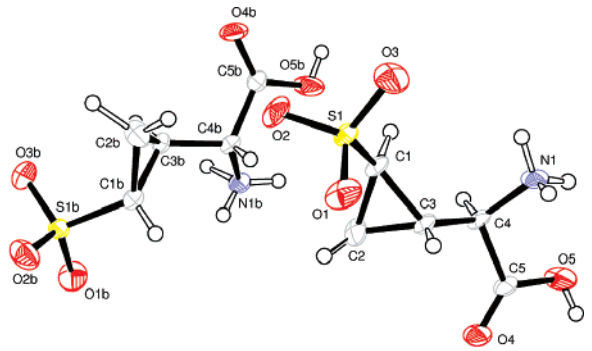

Figure 1. Drawing of compound *R*-SCG-1 (**10**) with the labeling of the atoms. The non-H-atom ellipsoids enclose 50% probability.

Absolute Configuration Assignment

The absolute configuration assignment to the eight diastereoisomeric amino acids **8**−**15** was based upon the single-crystal X-ray analysis performed on suitable selected compounds chosen among the final compounds derived from the two racemic aldehydes (±)-**26** and (±)-**27**, depending on the quality of their crystals. All the three structures crystallized in the same acentric space group (Monoclinic, $P2_1$), thus indicating their enantiomeric purity. Thus, X-ray analysis of the amino acid *R*-SCG-1 (**10**, Figure 1), derived from one of the two minor α-amino nitriles obtained from (±)-**26**, confirmed the *R*-chirality of the amino acidic center and allowed to fix the absolute configuration at the two cyclopropylic carbon atoms [(1′*S*, 2′*R*)]. Conversely, the compound *R*-SCG-2 (**11**), proceeding from the other minor α-amino nitrile **35**, resulted endowed with the same absolute configuration (*R*) at C-2 and opposite (1′*R*, 2′*S*) at cyclopropane. Moreover, a comparison of the specific rotatory powers of **10** and **11** with those of **8** and **9** revealed the corresponding couples of enantiomers.

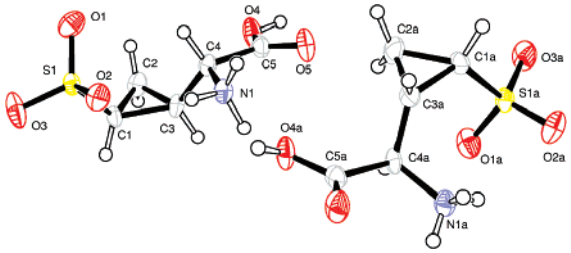

Figure 2. Drawing of the asymmetric unit of *R*-SCG-3 (**12**) with the labeling of the atoms. The non-H-atom ellipsoids enclose 50% probability.

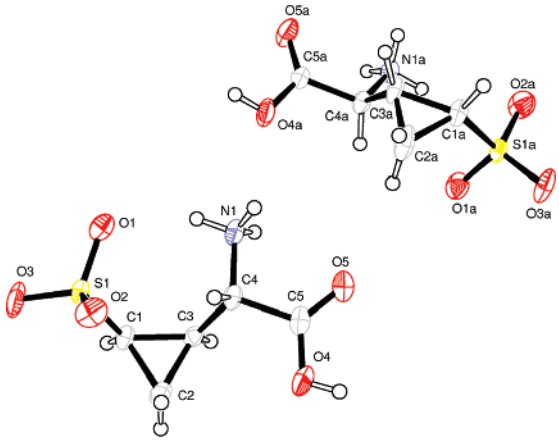

Figure 3. Drawing of the asymmetric unit of *S*-SCG-3 (**13**) with the labeling of the atoms. The non-H-atom ellipsoids enclose 50% probability.

In the case of the SCGs, obtained starting from racemic *cis*-aldehyde (±)-**27**, because it was not possible to identify unequivocally two major and two minor components in the mixture after Strecker reaction, X-ray analysis was performed on two amino acids among the four corresponding ones, resulting **12** and **13**, endowed with (2*R*,1′*S*,2′*S*)- and (2*S*,1′*R*,2′*R*)-absolute configurations, respectively (Figures 2 and 3). In both the cases, the asymmetric unit was formed by two crystallographic independent molecules. As above, the corresponding enantiomers were disclosed by the comparison of the specific rotatory power values.

Biological Results

The pharmacological profiles of the eight SCG isomers (**8**−**15**), compared to *L*-HCA (**18**) and *L*-Glu (**1**), were assessed by evaluating the inhibition of the binding of selective ligands both at AMPA, KA, and NMDA receptor channels and at mGlu1, mGluR2, mGluR4, and mGlu5 receptor subtypes (Table 1).

In agreement with previous studies,[41−46] we observed low μM activity of *L*-HCA (**18**) at iGluRs and higher μM affinity at mGluRs. The inspection of Table 1 reveals that within mGluRs, *S*-SCG-1 (**8**) selectively displaces labeled quisqualic acid from group I mGluRs at micromolar range. Interestingly, its enantiomer, *R*-SCG-1 (**10**), and *R*-SCG-4 (**14**) are both relatively selective but weak ligands at mGluR5 and moderately active ligands at iGluRs.

As far as iGluRs are concerned, Table 1 shows that many SCGs display sub-micromolar affinities at this class of receptors. Thus, both *S*-SCG-2 (**9**) and *R*-SCG-3 (**12**) displace labeled kainate at micromolar concentrations, but while **9** also weakly binds at group I mGluRs, *R*-SCG-3 (**12**) is a selective ligand of KA receptor. Among all SCG stereoisomers, *S*-SCG-4 (**15**) displays the most interesting pharmacological profile being

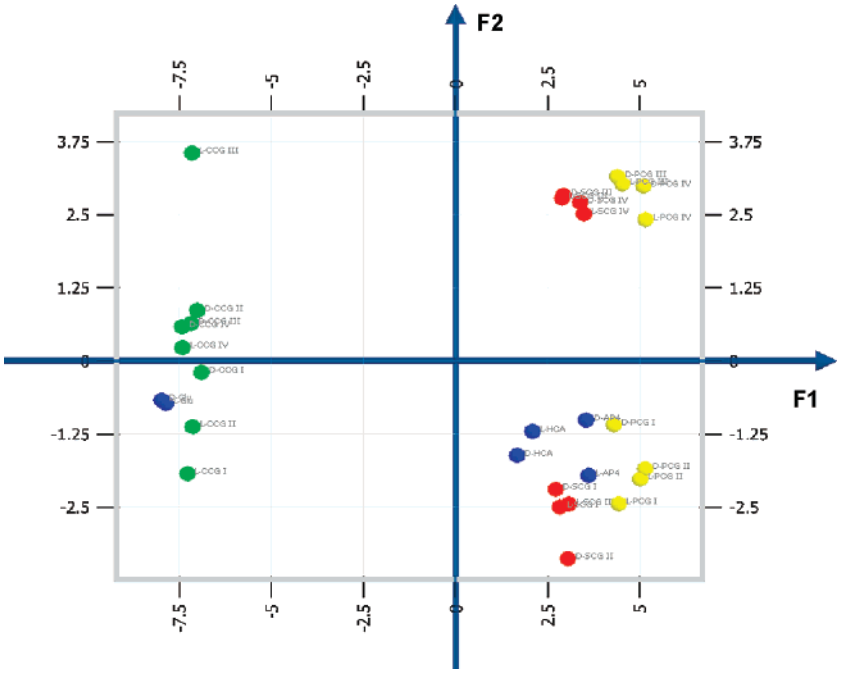

Figure 4. Plot of the first two components (F1, F2) of the principal component analysis (PCA). CCGs (green), PCGs (yellow), SCGs (red), and the respective linear templates (blue) are shown. For each class of compounds, all the possible enantiomers are plotted.

endowed with a very low micromolar affinity at AMPA receptor (0.10 μM) that is 1-fold and 2-fold more, respectively, than those at KA and NMDA receptor subtypes.

Molecular Modeling

Principal Component Analysis. To analyze the portion of chemical space occupied by SCGs (**8**−**15**) in respect to CCGs (Chart 1) and (phosphonocyclopropyl)glycines (PCGs, Chart 2), a principal component analysis (PCA) was carried out using a set of 40 molecular descriptors related to the electronic properties and size of molecular shape of each compound (Figure 4). In particular, charged partial surface area descriptors (30) and shadow indices descriptors (10) were calculated. While the first descriptors capture the electronic shape information of molecules, shadow indices are geometric descriptors that help to characterize the geometrical shape of the molecules. Both of them are intrinsically related to the pharmacokinetic and pharmacodynamic profiles of the compounds because both the charge distribution and the geometry of the molecular shape affect solubility, distribution, and the interaction with the biological target.

The inspection of the principal components reveals that the first two components (PC1 and PC2) explain about 83% of the variance of independent variables. The first component (PC1, Figure 4), in particular, discriminates the compounds of the three libraries according to the bioisosteric replacement of the distal carboxylic group of *L*-Glu (**1**). Thus, *L*-Glu (**1**) and CCGs (**2**−**5**) occupy negative values of PC1, while *L*-AP4, *L*-HCA (**18**), and their relative cyclopropyl constrained stereolibraries are shifted toward positive values of PC1.

The second component (PC2, Figure 4) differentiates compounds according to the conformational constrained geometry. In particular, compounds constrained in folded conformations occupy mostly the upper part of PC2, whereas compounds constrained in extended conformations assume generally lower values of PC2. Overall, PCA results indicate that SCGs (**8**−**15**) are located in a region of the chemical space that is unoccupied by CCGs, but close to the region occupied by PCGs.

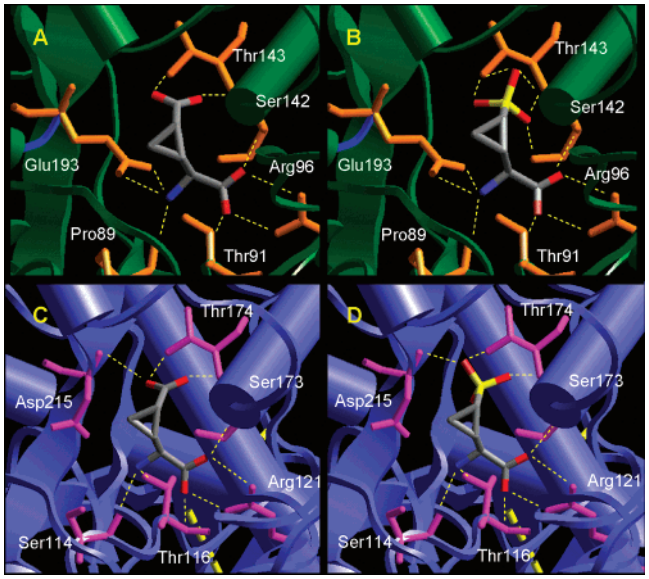

Figure 5. Docking results of *L*-CCG IV (**5**) (a, c) and *S*-SCG-4 (**15**) (b, d) into the binding sites of GluR2 (a, b) and NR2A (c, d).

Molecular Docking. Docking experiments of *S*-SCG-4 (**15**) and *L*-CCG IV (**5**) were carried out into the binding sites of GluR2 and NR2A. In the resulting binding poses, both compounds **5** and **15** adopt similar bioactive conformations and pattern of interaction (Figure 5). In particular, the amino acidic moieties of *S*-SCG-4 (**15**) and *L*-CCG IV (**5**) make electrostatic enforced hydrogen bonds with Arg96 and Glu193 in GluR2 and with Arg121 in NR2A. Interestingly, Asp215 in NR2A may form only electrostatic interactions with the α-amino group of the ligands. Additional hydrogen bonds are observed between the amino acidic moiety of the compounds and the side chain of Thr91 in GluR2, Thr116 in NR2A and the backbone of Pro89, Ser142 in GluR2 and Ser114, Ser173 in NR2A (Figure 5).

The presence of the sulfonic acid as the distal acidic group in *S*-SCG-4 (**15**) leads to additional hydrogen bonds than *L*-CCG IV (**5**) with the backbones and side chains of Ser142 and Thr143 in GluR2 (Table 2, Figure 5a,b). Interestingly, this trend is not

Table 2. Comparison of Some Energetical Parameters and Interaction Features between the Docking Poses of *L*-CCG-IV (**5**) and *S*-SCG-4 (**15**) in the AMPA-GluR2 and NMDA-NR2A Receptors

	AMPA-GluR2		NMDA-NR2A	
descriptors	*L*-CCG-IV (**5**)	*S*-SCG-4 (**15**)	*L*-CCG-IV (**5**)	*S*-SCG-4 (**15**)
number of hydrogen bonds involving the distal acidic group	2	5	3	3
docking energy (kcal/mol)	−9.95	−13.38	−8.74	−11.89
conformational gap energy (Δ*E*, kcal/mol)	5.0	1.4	1.6	2.0

observed in NR2A where the distal acidic groups of *L*-CCG IV (**5**) and *S*-SCG-4 (**15**) show a conserved pattern of three hydrogen bonds with the side chain of Thr174 and the backbones of Ser173 and Asp215 (Table 2, Figure 5c,d). These differences contribute to diverse docking energies observed among the binding poses of *L*-CCG IV (**5**) and *S*-SCG-4 (**15**) in GluR2 and NR2A (Table 2).

Moreover, different conformational gap energies are associated between the bioactive conformations of compounds **5**, **15**, and their relative global minimum conformation (Table 2, Figure 6). In the case of *L*-CCG IV (**5**), the conformation docked at GluR2 is endowed with a higher conformational gap energy (Δenergy = 5.0 kcal/mol) than the bioactive conformation binding at NR2A (Δenergy = 1.6 kcal/mol). Conversely, the nonplanar sulfonic acid of *S*-SCG-4 (**15**) allows to adopt bioactive conformations nearby the global minimum both in the binding site of GluR2 and NR2A (GluR2 Δenergy = 1.4 kcal/mol; NR2A Δenergy = 2.0 kcal/mol).

Discussion

The endogenous metabolite *L*-HCA (**18**) can be envisaged as a natural occurring bioisoster of *L*-Glu (**1**). Interestingly, experimental evidence pinpoints the physiological importance of this metabolite in the brain as a gliotransmitter in mediating signaling between glial cells and neuronal synapses through the activation of both iGluRs and mGluRs. On the basis of these observations, *L*-HCA (**18**) can be considered a good lead compound to design novel glutamatergic modulators.

Thus, with the aim of providing novel chemical tools to characterize glutamatergic as well as ESAAs pathways in the brain and as a continuation of our work devoted to the preparation of cyclopropyl-constrained glutamate analogs, we synthesized a library of eight stereoisomers based on the introduction of a cyclopropyl ring in the β and γ carbons of the *L*-HCA backbone.

The introduction of such a ring moiety on the HCA skeleton allows (i) a partial reduction in the conformational flexibility of the molecule to achieve a selective molecular recognition by a reduced number of receptor subtypes, and (ii) assessment of the bioactive conformation of the molecule acting at a given receptor subtype through the specific orientation of functional groups around the cyclopropyl moiety of the active stereoisomer.

As a general consideration, the synthesis of SCGs (**8**−**15**) allows a portion of the chemical space to be explored, as resulting in the PCA study (Figure 4), that is unoccupied by CCGs (Chart 1), but close to the region occupied by PCGs (Chart 2).

In particular, the differentiation of the compounds along the first principal component (PC1, Figure 4) reflects the bioisosteric relationships existing among carboxylic, sulfonic, and phosphonic acidic groups. Sulfonic and phosphonic acids, indeed,

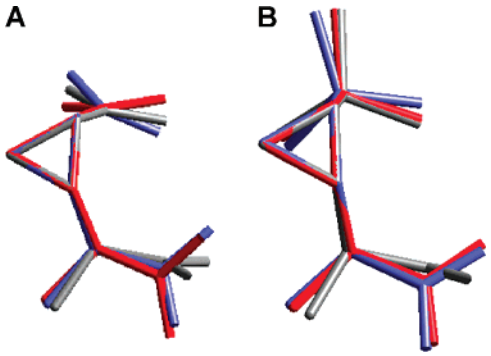

Figure 6. (a) Superposition of the GluR2 (red) and NR2A (blue) bioactive conformations of *L*-CCG IV (**5**) on the global minimum conformation (gray). (b) Superposition of the GluR2 (red) and NR2A (blue) bioactive conformations of *S*-SCG-4 (**15**) on the global minimum conformation (gray).

have been classified as nonplanar bioisosteric surrogates of the carboxylic acidic function.[47] Sulfonic and phosphonic groups, in particular, share a pyramidal geometry around the central sulfur and phosphorus atom, whereas the carboxylic group displays a planar geometry. Although all the three acidic groups may form both electrostatic interactions and hydrogen bonding, differences exist in their preferred geometries of the hydrogen bond interactions. The carboxylic group, in particular, prefers hydrogen bond interactions along the lone-pairs in the *syn*-position,[48−50] the sulfonic group adopts a nearly *eclipsed* geometry of the hydrogen bond interaction angle, whereas the phosphonic group prefers a *gauche* orientation of the interaction angle.[51] In addition, a crystallographic database survey of geometrical features of the hydrogen bonding interactions pinpoints that the sulfonic group tends to form longer interactions then the carboxylic and phosphonic groups.[52]

Conversely, the separation of the compounds along the second principal component (PC2, Figure 4) is associated with the presence of a folded or extended conformational geometry between the amino acidic moiety and the distal acidic group. In this context, it is worth noting how the pharmacological evaluation of CCGs (**2**−**5**) allowed the definition of the bioactive conformations of *L*-Glu (**1**) acting at iGluRs and mGluRs when the crystal structures of the ligand binding domains of these receptors were still missing.[3,53,54.]

Thus, while the strong agonistic activity of *L*-CCG IV (**5**) at NMDA receptor pinpointed a folded bioactive conformation of *L*-Glu as acting at iGluRs, the ability of *L*-CCG I (**2**) to activate mGluR1 highlighted an extended bioactive conformation of *L*-Glu as acting at mGluRs.

Analogously, the pharmacological evaluation of the eight diastereoisomeric SCGs (**8**−**15**) at iGluRs and mGluRs indicates that the same trend is conserved by the folded *S*-SCG-4 (**15**), which possesses an interesting profile at iGluRs, and by the extended *S*-SCG-1 (**8**), which displays a better activity at mGluRs (Table 1). The only exceptions to that rule are both the extended *S*- and *R*-stereoisomers of SCG-2 (**9** and **11**, respectively), which are moderately active at KA receptors.

More in detail, among the active compounds, *S*-SCG-4 (**15**) displays the most potent affinity at the AMPA receptor. Interestingly, it shows a different order of potency compared to its corresponding carboxylic bioisoster, namely, *L*-CCG IV (**5**), which is a potent and selective agonist at the NMDA receptor (K_i = 0.009 μM).[3] To investigate the structural and conformational features underlying the pharmacological properties of *S*-SCG-4 (**15**) and *L*-CCG IV (**5**), we carried out docking experiments of these compounds into the AMPA and NMDA

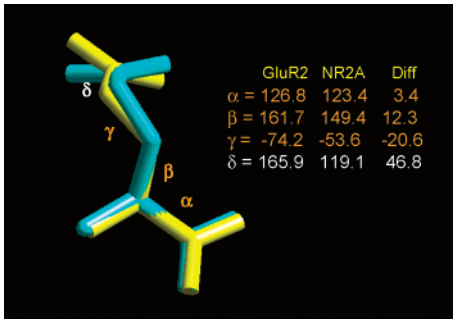

Figure 7. Different folded bioactive conformations of *L*-Glu (**1**) binding AMPA-GluR2 (yellow) and NMDA-NR2A (cyan) receptors as observed in the crystal structures of the ligand binding domains.

receptors. These computational experiments, in particular, were performed using the available crystal structures of the ligand binding domains of NMDA-NR2A and AMPA-GluR2 receptor subtypes.[55,56]

The inspection of these crystal structures in complex with *L*-Glu reveals that two different folded bioactive conformations of glutamate bind, respectively, NMDA and AMPA receptors (Figure 7).

More in detail, the bioactive conformations of *L*-Glu (**1**) at NR2A and GluR2 are both endowed with a fold rearrangement of the N−Cα−Cβ−Cγ torsional angle. Interestingly, the angle defined by the atoms Cβ−Cγ−C_O−O_{E1} is 119.1° in NR2A, while it adopts a value of 165.9° in GluR2.

This is probably ascribed to the subtle difference existing between the binding sites of the distal carboxylic group of *L*-Glu (**1**) in the two receptors, which consists of a residue of Asp215 present in NR2A that is replaced by a residue of Glu193 in the GluR2 subtype. The longer residue of Glu193 in the AMPA receptor may indeed force a conformational strain of the Cβ−Cγ−C_O−O_{E1} torsional angle to accommodate the ligand.

Docking experiments reveal that both *S*-SCG-4 (**15**) and *L*-CCG IV (**5**) adopt similar binding poses in GluR2 and NR2A (Figure 5).

Nevertheless, different docking and conformational gap energies are associated with the bioactive conformations of compounds **5** and **15** docked into the binding site of GluR2 and NR2A (Table 2).

These differences of energy explain the better activity of *L*-CCG IV (**5**) at NMDA over AMPA receptor and the preferred activity of *S*-SCG-4 (**15**) at AMPA receptor. In particular, the conformation of *L*-CCG IV (**5**) docked at GluR2 is endowed with a higher conformational gap energy (Δenergy = 5.0 kcal/mol) than the bioactive conformation docked at NR2A (Δenergy = 1.6 kcal/mol). This is not the case of *S*-SCG-4 (**15**) in which the nonplanar sulfonic moiety allows the adoption of a bioactive conformation nearby the global minimum both in the binding site of GluR2 and in the binding site of NR2A (GluR2 Δenergy = 1.4 kcal/mol; NR2A Δenergy = 2.0 kcal/mol).

The origin of the preferred binding of *S*-SCG-4 (**15**) at AMPA receptor relies on the higher number of hydrogen bond interactions and better docking energy that this compound forms in the binding site of AMPA receptor (AMPA $E_{docking}$ = −13.38 kcal/mol; NMDA $E_{docking}$ = −11.89 kcal/mol). Briefly, in the docked pose of AMPA receptor, **15** is pushed toward Thr143 and Ser142 by the presence of the negatively bulky side chain of Glu193 (Figure 5b); here, the sulfonic moiety of *S*-SCG-4 (**15**) is forced to form a network of five hydrogen bonds with the polar hydrogen atoms of Thr143 and Ser142. Conversely, the presence of Asp215 in the NMDA receptor allows **15** to adopt a docking pose where its sulfonic moiety forms only three

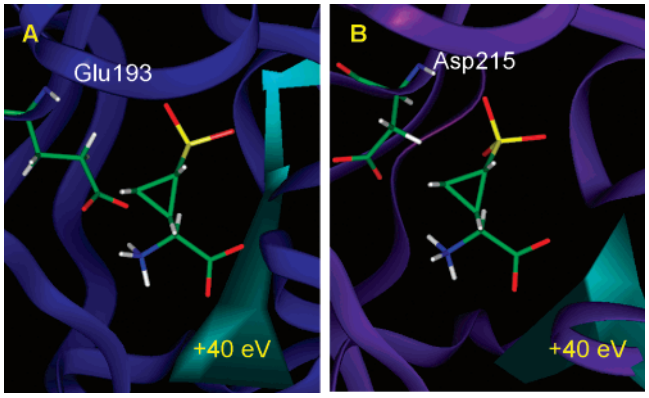

Figure 8. Electrostatic potential maps inside the binding site of GluR2 (a) and NR2A (b) contoured at level +40 eV (cyan).

hydrogen bonds with the side chain of Thr174 and the backbone of Asp215 (Figure 5d).

From the inspection of Table 2, however, it is not clear the origin of the weak affinity of *S*-SCG-4 (**15**, K_i = 19 μM) with respect to *L*-CCG IV (**5**, K_i = 0.009 μM) at NMDA receptor. One could argue that the presence of the shorter Asp215 in the NMDA receptor, which is not directly salt bridged to the α-amino group of the ligand (distance of interaction measured between the nitrogen of the α-amino group and the χ-carbon of Asp215 side chain = 4.29 Å) defines a more acidic pH environment around the distal acidic moiety of the ligand. This is in part evidenced by the comparison of the molecular electrostatic potential inside the binding site of both receptors (Figure 8).

The AMPA-GluR2 receptor displays, indeed, a wider positive electrostatic potential (contour level +40 eV) then the NMDA-NR2A receptor around the distal acidic moiety of the ligand.

Thus, the difference of potency between *L*-CCG IV (**5**) and *S*-SCG-4 (**15**) could be explained by different pK_a values of the distal carboxylic acid group (calculated pK_a = 4.12) and sulfonic acid group (calculated pK_a = −1.30) that affect the protonation state of the molecules into the binding site of the receptor. In the presence of the acidic pH environment of NMDA-NR2A, compound **15** would be still negatively charged, whereas compound **5** would be protonated having a formal charge of 0. The absence of a net negative charge on the distal acidic group of *L*-CCG IV (**5**) would damp possible electrostatic repulsions with the negatively charged side chain of Asp215 favoring the binding at NMDA receptor subtype (Figure 8).

Conclusion

In this paper we have reported the synthesis of the first stereolibrary of conformationally constrained analogs of *L*-HCA (**18**).

Preliminary pharmacological characterizations of the eight stereoisomers of SCGs **(8-15)** indicate that some of them are able to interact in the low micromolar range with mGlu1 receptor (*S*-SCG-1, **8**), NMDA [*R*-SCG-2 (**11**) and *S*-SCG-4 (**15**)], kainate [*S*-SCG-2 (**9**), *R*-SCG-2 (**11**), *R*-SCG-3 (**12**), and *S*-SCG-4 (**15**)], and AMPA receptor [*S*-SCG-4 (**15**)]. Among the active compounds, *S*-SCG-4 (**15**) demonstrates the ability to be a potent and relatively selective AMPA ligand with an inhibitory constant (K_i) of 0.10 μM.

Docking experiments of *S*-SCG-4 (**15**) into the ligand binding domains of AMPA-GluR2 and NMDA-NR2A, coupled to molecular electrostatic potential calculations, allow insight into the structural and conformational features underlying the pharmacological properties of this compound to be gained. In

particular, both the nonplanar geometry of the sulfonic moiety and the wide positive electrostatic potential of the binsing site, favor a strong interaction between **15** and AMPA receptor.

The reported stereolibrary of SCGs (**8**−**15**), while providing a novel source of modulators of the gluatamate receptors, represents a valuable chemical tool to better characterize *L*-HCA pathways in the CNS.

Experimental Section

General Methods. Melting points were determined by the capillary method on a Büchi 535 electrothermal apparatus and are uncorrected. ^{1}H and ^{13}C NMR spectra were taken on a Bruker AC 200 or Bruker AC 400 spectrometers as solutions in $CDCl_3$ unless otherwise indicated. The spin multiplicities are indicated by the symbols s (singlet), d (doublet), t (triplet), q (quartet), m (multiplet), and b (broad). GC MS was performed on a Hewlett-Packard HP 5890 gas chromatograph (column and conditions: HP-1, 12 m, 0.20 mm i.d., 0.33 μm ft, 150(1′)/280 °C, 10 °C/min) equipped with a mass detector (HP 5971). Flash chromatography was performed on Merck silica gel (0.040−0.063 mm). Medium-pressure chromatography (MPC) was performed on Merck LiChroprep Si 60 lobar columns. Optical rotations were recorded on a Jasco Dip-360 digital polarimeter. Microanalyses were carried out on a Carlo Erba 1106 elemental analyzer.

Neopentyl 2-[(1′*Z*)-Prop-1′-enyl]cyclopropanesulfonates (22−**25).** A solution of neopentyl diazomethanesulfonate (**20**, 0.70 g, 3.6 mmol) in 1,3-pentadiene (mixture of isomers; **21**, 5.0 mL) was added dropwise to a magnetically stirred suspension of copper(I) trifluoromethanesulfonate benzene complex (0.042 g, 0.08 mmol) in **19** (5.0 mL) kept under an argon atmosphere. After the addition was complete, the reaction mixture was stirred under argon at room temperature for 20 min. The reaction mixture was then evaporated and the residue was submitted to flash chromatography; elution with light petroleum−AcOEt (90:10) afforded the mixture (±)-**22** + (±)-**23** (0.27 g, 32%): ^{1}H NMR (200 MHz) δ 0.90 (9H, s, $C(CH_3)_3$ of both the isomers), 1.04 (1H, m, 3-CH_a of both the isomers), 1.45 (1H, m, 3-CH_b of both the isomers), 1.58 (2.1H, dd, J = 1.6, 6.5 Hz, 3′-CH_3 of major isomer), 1.67 (0.9H, dd, J = 1.7, 8.6 Hz, 3′-CH_3 of minor isomer), 2.20 (0.7H, m, 2-CH of major isomer), 2.29 (1.3H, m, 1-CH of both the isomers and 2-CH of minor isomer), 3.77 (2H, 2s, $SO_3CH_2C(CH_3)_3$ of both the isomers), 4.78−4.93 (0.3H, m, 1′-CH of minor isomer), 5.02−5.15 (0.7H, m, 1′-CH of major isomer), 5−58-5.81 (1H, m, 2′-CH of both the isomers); ^{13}C NMR (50 MHz) δ 11.64, 12.54, 17.77, 21.72, 26.03, 30.93, 31,75, 33.98, 34.34, 79.04, 79.45, 127.29, 127.64, 127.85, 128.22. Following elution with the same solvents gave the mixture (±)-**24** + (±)-**25** (0.35 g, 42%): ^{1}H NMR (200 MHz) δ 1.00 (9H, s, $C(CH_3)_3$ of both the isomers), 1.50 (2H, m, 3-CH_2 of both the isomers), 1.75 (3H, m, 3′-CH_3 of both the isomers), 2.05 (0.75H, m, 2-CH of major isomer), 2.30 (0.3H, m, 2-CH of minor isomer), 2−60-2.80 (1H, m, 1-CH of both the isomers), 3.90 (2H, m, $SO_3CH_2C(CH_3)_3$ of both the isomers), 5.40−5.85 (2H, m, 1′-CH and 2′-CH of both the isomers); ^{13}C NMR (50 MHz) δ 13.23, 13.59, 17.54, 17.95, 22.52, 26.05, 31.67, 34.12, 34.45, 78.97, 81.70, 125.15, 125.88, 128.06, 129.41.

(±)-(1*S*,2*R*)-Neopentyl 2-Formylcyclopropanesulfonate (26). Ozone was bubbled through a stirred solution of the mixture (±)-**22** + (±)-**23** (0.46 g, 1.98 mmol) in dichloromethane (75 mL) and cooled (−78 °C) until a persistent light blue color appeared. Dimethylsulfide (2.50 g, 40.80 mmol) was then added and the reaction was allowed to warm to room temperature. The solvent was removed in vacuo, yielding a residue that was purified by flash chromatography. Elution with light petroleum−AcOEt (60:40) gave (±)-**26** (0.30 g, 66%): ^{1}H NMR (200 MHz) δ 0.94 (9H, s, $C(CH_3)_3$), 1.64−1.86 (2H, m, 3-CH_2), 2.70 (1H, dddd, J = 2.5, 4.1, 5.9 and 8.7 Hz, 2-CH), 3.12 (1H, ddd, J = 4.1, 5.9 and 8.7 Hz, 1-CH), 3.86 (s, 2H, $SO_3CH_2C(CH_3)_3$), 9.58 (1H, d, J = 2.5 Hz, CHO); ^{13}C NMR (50 MHz) δ 13.69, 25.92, 26.70, 31.74, 34.97, 80.15, 196.15.

(±)-(1*S*,2*S*)-Neopentyl 2-Formylcyclopropanesulfonate (27). Ozone was bubbled through a stirred solution of the mixture (±)-**24** + (±)-**25** (0.46 g, 1.98 mmol) in dichloromethane (75 mL) and cooled (−78 °C) until a persistent light blue color appeared. Dimethylsulfide (2.50 g, 40.80 mmol) was then added and the reaction was allowed to warm to room temperature. The solvent was removed in vacuo, yielding a residue that was purified by flash chromatography. Elution with light petroleum−AcOEt (60:40) gave (±)-**27** (0.32 g, 72%): ^{1}H NMR (200 MHz) δ 0.94 (9H, s, $C(CH_3)_3$), 1.67−1.79 (1H, m, 3-CH_a), 2.08−2.21 (2H, m, 2-CH and 3-CH_b), 2.90−3.01 (1H, m, 1-CH), 3.85 (s, 2H, $SO_3CH_2C(CH_3)_3$), 9.35 (1H, d, J = 6.4 Hz, CHO); ^{13}C NMR (50 MHz) δ 12.11, 25.93, 29.22, 31.74, 35.91, 79.93, 196.71.

General Procedure for the Stereoselective Strecker Synthesis to Give Substituted α-Amino Nitriles. (*R*)-α-Phenylglycinol (2.70 mmol) was added to a solution of the aldehyde (2.67 mmol) in methanol (30 mL), and the resulting solution was magnetically stirred at room temperature for 4 h. After cooling to 0 °C, TMSCN (5.34 mmol) was added, and the resulting mixture was stirred for 12 h at room temperature. Evaporation of the solvent gave a residue that was submitted to medium-pressure chromatography using hexane−AcOEt mixtures as eluent to give the corresponding *N*-substituted α-amino nitriles.

(2*S*,1′*R*,2′*S*)-*N*-[(*R*)-α-Phenylglycinyl]-2-(2′-neopentyloxysulfonylcyclopropyl)glycinonitrile (32). *n*-Hexane−AcOEt (75:25); 15% yield; ^{1}H NMR (200 MHz) δ 0.94 (9H, s, $C(CH_3)_3$), 1.16−1.31 (1H, m, 3′-CH_a), 1.45−1.56 (1H, m, 3′-CH_b), 1.99−2.11 (1H, m, 1′-CH), 2.45−2.54 (1H, m, 2′-CH), 3.35 (1H, d, J = 6.2 Hz, CHCN), 3.57 (1H, dd, J = 9.5 and 10.7 Hz, CH_aOH), 3.75 (1H, dd, J = 3.8 and 10.7 Hz, CH_bOH), 3.88 (2H, 2s, $SO_3CH_2C(CH_3)_3$), 4.00−4.11 (1H, m, C*H*Ph), 7.30 (s, 5H, aromatics); ^{13}C NMR (50 MHz) δ 9.86, 20.68, 25.97, 31.57, 31.78, 48.63, 62.99, 66.94, 79.87, 116.94, 127.61, 128.76, 129.11, 137.01; $[\alpha]^{20}_D$ −63.93 (*c* 1.50, $CHCl_3$).

(2*S*,1′*S*,2′*R*)-*N*-[(*R*)-α-Phenylglycinyl]-2-(2′-neopentyloxysulfonylcyclopropyl)glycinonitrile (33). *n*-Hexane−AcOEt (75:25); 21% yield; ^{1}H NMR (200 MHz) δ 0.93 (9H, s, $C(CH_3)_3$), 1.16−1.28 (1H, m, 3′-CH_a), 1.44−1.55 (1H, m, 3′-CH_b), 1.99−2.12 (1H, m, 1′-CH), 2.58−2.68 (1H, m, 2′-CH), 3.48 (1H, d, J = 5.4 Hz, CHCN), 3.58 (1H, dd, J = 9.5 and 10.7 Hz, CH_aOH), 3.76 (1H, dd, J = 4.0 and 10.7 Hz, CH_bOH), 3.88 (2H, 2s, $SO_3CH_2C(CH_3)_3$), 4.05 (1H, dd, J = 4.0 and 9.5 Hz, C*H*Ph), 7.30 (s, 5H, aromatics); ^{13}C NMR (50 MHz) δ 9.89, 20.97, 25.94, 30.68, 31.75, 48.11, 62.97, 66.94, 79.80, 117.31, 127.61, 128.52, 128.99, 137.69; $[\alpha]^{20}_D$ −133.00 (*c* 1.53, $CHCl_3$).

(2*R*,1′*S*,2′*R*)-*N*-[(*R*)-α-Phenylglycinyl]-2-(2′-neopentyloxysulfonylcyclopropyl)glycinonitrile (34). *n*-Hexane−AcOEt (75:25); 6% yield; ^{1}H NMR (200 MHz) δ 0.92 (9H, s, $C(CH_3)_3$), 1.18−1.29 (1H, m, 3′-CH_a), 1.43−1.53 (1H, m, 3′-CH_b), 1.93−2.06 (1H, m, 1′-CH), 2.52−2.61 (1H, m, 2′-CH), 3.57 (1H, dd, J = 8.0 and 11.0 Hz, CH_aOH), 3.70 (1H, dd, J = 4.0 and 11.0 Hz, CH_bOH), 3.80 (1H, d, J = 6.2 Hz, CHCN), 3.88 (2H, 2s, $SO_3CH_2C(CH_3)_3$), 3.98 (1H, dd, J = 4.0 and 8.0 Hz, C*H*Ph), 7.30 (s, 5H, aromatics); ^{13}C NMR (50 MHz) δ 11.10, 20.95, 25.93, 30.75, 31.77, 49.06, 62.63, 66.88, 79.86, 117.39, 127.41, 128.48, 128.93, 138.52; $[\alpha]^{20}_D$ −8.61 (*c* 2.85, $CHCl_3$).

(2*R*,1′*R*,2′*S*)-*N*-[(*R*)-α-Phenylglycinyl]-2-(2′-neopentyloxysulfonylcyclopropyl)glycinonitrile (35). *n*-Hexane−AcOEt (75:25); 7% yield; ^{1}H NMR (200 MHz) δ 0.93 (9H, s, $C(CH_3)_3$), 1.08−1.23 (1H, m, 3′-CH_a), 1.29−1.39 (1H, m, 3′-CH_b), 1.87−2.00 (1H, m, 1′-CH), 2.43−2.52 (1H, m, 2′-CH), 3.57 (1H, dd, J = 8.2 and 11.0 Hz, CH_aOH), 3.70 (1H, dd, J = 4.0 and 11.0 Hz, CH_bOH), 3.78 (1H, d, J = 6.2 Hz, CHCN), 3.88 (2H, s, $SO_3CH_2C(CH_3)_3$), 4.03 (1H, dd, J = 4.0 and 8.2 Hz, C*H*Ph), 7.30 (s, 5H, aromatics); ^{13}C NMR (50 MHz) δ 9.63, 20.87, 25.95, 31.77, 32.23, 49.55, 62.48, 66.96, 79.82, 117.33, 127.44, 128.45, 128.95, 138.61; $[\alpha]^{20}_D$ −56.29 (*c* 4.00, $CHCl_3$).

(2*R*,1′*S*,2′*S*)-*N*-[(*R*)-α-Phenylglycinyl]-2-(2′-neopentyloxysulfonylcyclopropyl)glycinonitrile (36). Light petroleum−acetone (85:15); 34% yield; ^{1}H NMR (200 MHz) 0.95 (9H, s, $C(CH_3)_3$), 1.41−1.51 (2H, m, 3′-CH_2), 1.62−1.79 (1H, m, 1′-CH), 2.46−

2.58 (1H, m, 2′-CH), 3.08 (1H, dd, J = 7.4 and 11.6 Hz, CH_aOH), 3.72 (1H, dd, J = 3.8 and 11.6 Hz, CH_bOH), 3.91 (2H, s, $SO_3CH_2C(CH_3)_3$), 3.94 (1H, dd, J = 3.8 and 7.4 Hz, CHPh), 4.06 (1H, d, J = 10.6 Hz, CHCN), 7.30 (s, 5H, aromatics); ^{13}C NMR (50 MHz) δ 11.65, 23.20, 26.04, 31.89, 32.52, 48.06, 63.66, 65.89, 80.32, 118.82, 127.54, 128.26, 128.74, 139.63; $[\alpha]^{20}_D$ −2.63 (*c* 0.72, $CHCl_3$).

(2*S*,1′*R*,2′*R*)-*N*-[(*R*)-α-Phenylglycinyl]-2-(2′-neopentyloxysulfonylcyclopropyl)glycinonitrile (37). Light petroleum−acetone (85:15); 29% yield; ^{1}H NMR (200 MHz) 0.92 (s, 9H, $C(CH_3)_3$), 1.26−1.33 (1H, m, 3′-CH_a), 1.37−1.47 (1H, m, 3′-CH_b), 1.75−1.95 (1H, m, 1′-CH), 2.53−2.68 (1H, m, 2′-CH), 3.57 (1H, dd, J = 9.0 and 10.8 Hz, CH_aOH), 3.68−3.79 (3H, m, CH_bOH and CHCN), 3.84 (2H, 2s, $SO_3CH_2C(CH_3)_3$), 4.06 (1H, dd, J = 4.2 and 9.0 Hz, CHPh), 7.28 (5H, m, aromatics);^{13}C NMR (50 MHz) δ 10.76, 22.47, 26.05, 31.83, 32.49, 46.67, 63.02, 67.13, 80.29, 118.52, 128.00, 128.39, 128.71, 137.18; $[\alpha]^{20}_D$ −94.55 (*c* 1.68, $CHCl_3$).

(2*R*,1′*R*,2′*R*)-*N*-[(*R*)-α-Phenylglycinyl]-2-(2′-neopentyloxysulfonylcyclopropyl)glycinonitrile (38). Light petroleum−acetone (85:15); 4% yield; ^{1}H NMR (200 MHz) δ 0.93 (9H, s, $C(CH_3)_3$), 1.11−1.54 (3H, m, 1′-CH and 3′-CH_2), 2.50−2.61 (1H, m, 2′-CH), 3.62 (1H, dd, J = 8.2 and 11.0, CH_aOH), 3.72 (1H, m, J = 4.0 and 11.0 Hz, CH_bOH), 3.88 (2H, s, $SO_3CH_2C(CH_3)_3$), 4.04−4.14 (2H, m, CHCN and CHPh), 7.30 (5H, m, aromatics);^{13}C NMR (50 MHz) δ 12.10, 23.27, 26.04, 31.79, 32.78, 46.32, 62.62, 66.51, 79.70, 118.74, 127.54, 128.43, 128.86, 139.19; $[\alpha]^{20}_D$ −86.83 (*c* 0.66, $CHCl_3$).

(2*S*,1′*S*,2′*S*)-*N*-[(*R*)-α-Phenylglycinyl]-2-(2′-neopentyloxysulfonylcyclopropyl)glycinonitrile (39). Light petroleum−acetone (85:15); 15% yield; ^{1}H NMR (400 MHz) 0.98 (9H, s, $C(CH_3)_3$), 1.31−1.36 (1H, m, 3′-CH_a), 1.49−1.55 (1H, m, 3′-CH_b), 1.84−1.92 (1H, m, 1′-CH), 2.68−2.74 (1H, m, 2′-CH), 3.62 (1H, dd, J = 9.4 and 10.8, CH_aOH), 3.66 (1H, d, J = 10.4 Hz, CHCN), 3.80 (1H, dd, J = 3.9 and 10.8 Hz, CH_bOH), 3.90 (2H, s, $SO_3CH_2C(CH_3)_3$), 4.14 (1H, dd, J = 3.9 and 6.1 Hz, CHPh), 7.35 (5H, m, aromatics); ^{13}C NMR (100 MHz) δ 12.49, 23.48, 26.56, 32.32, 33.35, 46.28, 54.18, 63.72, 68.06, 80.47, 120.18, 128.64, 129.68, 130.13, 138.89; $[\alpha]^{20}_D$ −102.63 (*c* 1.97, $CHCl_3$).

General Procedure for the Oxidative Cleavage and Hydrolysis of *N*-Substituted α-Amino Nitriles. Lead(IV) acetate (0.49 mmol) was added to a cold (0 °C), magnetically stirred solution of the nitrile (0.41 mmol) in anhydrous MeOH/CH_2Cl_2 (1:2, 24 mL). After 7 h, phosphate buffer (pH 7.7, 12 mL) was added and the resulting mixture was filtered with the aid of Celite. After evaporation of the solvent, the residue was heated at 95 °C in 6 N HCl (5 mL) for 18−24 h. The reaction mixture was evaporated to dryness and the residue was submitted to ion-exchange resin chromatography (Dowex 1X8-200).

(2*S*,1′*R*,2′*S*)-2-(2′-Sulfonocyclopropyl)glycine (*S*-SCG-1, 8). HCl (1 N); 32% yield; ^{1}H NMR (400 MHz, D_2O) δ 1.24−1.35 (2H, m, 3′-CH_2), 1.70−1.77(1H, m, 1′-CH), 2.58−2.64 (1H, m, 2′-CH), 3.56 (1H, d, J = 10.0 Hz, 2-CH); ^{13}C NMR (100 MHz, D_2O) δ 10.40, 18.33, 33.91, 54.69, 170.43; $[\alpha]^{20}_D$ + 107.14° (c 1.55, H_2O); Anal. Calcd for $C_5H_9NO_5S$: C, 30.77; H, 4.65; N, 7.18. Found: C, 30.79; H, 4.65; N, 7.20.

(2*S*,1′*S*,2′*R*)-2-(2′-Sulfonocyclopropyl)glycine (*S*-SCG-2, 9). HCl (1 N); 40% yield; ^{1}H NMR (400 MHz, D_2O) δ 1.11−1.16 (1H, m, 3′-CH_a), 1.23−1.28 (1H, m, 3′-CH_b), 1.64−1.70 (1H, m, 1′-CH), 2.65−2.70 (1H, m, 2′-CH), 3.55 (1H, d, J = 10.0 Hz, 2-CH); ^{13}C NMR (100 MHz, D_2O) δ 10.78, 18.63, 34.60, 55.05, 170.75; $[\alpha]^{20}_D$ + 14.13° (*c* 2.65, H_2O); Anal. Calcd for $C_5H_9NO_5S$: C, 30.77; H, 4.65; N, 7.18. Found: C, 30.83; H, 4.67; N, 7.22.

(2*R*,1′*S*,2′*R*)-2-(2′-Sulfonocyclopropyl)glycine (*R*-SCG-1, 10). HCl (1 N); 45% yield; $[\alpha]^{20}_D$ −168.40° (*c* 0.43, H_2O); Anal. Calcd for $C_5H_9NO_5S$: C, 30.77; H, 4.65; N, 7.18. Found: C, 30.81; H, 4.67; N, 7.22.

(2*R*,1′*R*,2′*S*)-2-(2′-Sulfonocyclopropyl)glycine (*R*-SCG-2, 11). HCl (1 N); 45% yield; $[\alpha]^{20}_D$ −16.10° (*c* 0.41, H_2O); Anal. Calcd for $C_5H_9NO_5S$: C, 30.77; H, 4.65; N, 7.18. Found: C, 30.84; H, 4.68; N, 7.23.

(2*R*,1′*S*,2′*S*)-2-(2′-Sulfonocyclopropyl)glycine (*R*-SCG-3, 12). HCl (1 N); 47% yield; ^{1}H NMR (D_2O) δ 1.20−1.34 (2H, m, 3′-CH_2), 1.43−1.58 (1H, m, 1′-CH), 2.44−2.56 (1H, m, 2′-CH), 4.98 (1H, d, J = 11.0 Hz, 2-CH); ^{13}C NMR (50 MHz, D_2O) δ 11.52, 17.66, 33.19, 52.56, 181.16; $[\alpha]^{20}_D$ −20.00° (*c* 0.60, H_2O); Anal. Calcd for $C_5H_9NO_5S$: C, 30.77; H, 4.65; N, 7.18. Found: C, 30.78; H, 4.65; N, 7.19.

(2*S*,1′*R*,2′*R*)-2-(2′-Sulfonocyclopropyl)glycine (*S*-SCG-3, 13). HCl (1 N); 58% yield; $[\alpha]^{20}_D$ + 24.65° (c 0.61, H_2O); Anal. Calcd for $C_5H_9NO_5S$: C, 30.77; H, 4.65; N, 7.18. Found: C, 30.85; H, 4.68; N, 7.22.

(2*R*,1′*R*,2′*R*)-2-(2′-Sulfonocyclopropyl)glycine (*R*-SCG-4, 14). HCl (1 N); 53% yield; ^{1}H NMR (D_2O) δ 0.94−1.01 (1H, m, 3′-CH_a), 1.12−1.24 (1H, m, 3′-CH_b), 1.49−1.58 (1H, m, 1′-CH), 2.43−2.50 (1H, m, 2′-CH), 4.27 (1H, d, J = 10.6 Hz, 2-CH); ^{13}C NMR (50 MHz, D_2O) δ 9.23, 18.53, 34.18, 50.69, 170.74; $[\alpha]^{20}_D$ −54.6° (*c* 0.69, H_2O); Anal. Calcd for $C_5H_9NO_5S$: C, 30.77; H, 4.65; N, 7.18. Found: C, 30.80; H, 4.67; N, 7.21.

(2*S*,1′*S*,2′*S*)-2-(2′-Sulfonocyclopropyl)glycine (*S*-SCG-4, 15). HCl (1 N); 50% yield; $[\alpha]^{20}_D$ 59.7° (c 0.66, H_2O); Anal. Calcd for $C_5H_9NO_5S$: C, 30.77; H, 4.65; N, 7.18. Found: C, 30.86; H, 4.68; N, 7.21.

(±)-Neopentyl 2-oxiran-2-yl-ethanesulfonate (30). A solution of **29** (1.40 g, 7.30 mmol) in CH_2Cl_2 (40 mL) was added to a stirred solution of 77% *m*-chloroperbenzoic acid (1.63 g, 7.30 mmol) in CH_2Cl_2 (28 mL) kept at room temperature. After 72 h, the excess of peracid was destroyed by the addition of 10% Na_2SO_3 (30 mL). The organic phase was separated, washed with 5% $NaHCO_3$ (40 mL) and then with water (40 mL), and dried (Na_2SO_4). The solvent was removed in vacuo to give a residue that was purified by flash chromatography. Elution with light petroleum−EtOAc (8:2) gave (±)-**30** (0.93 g, 61%). ^{1}H NMR (200 MHz) δ 0.93 (9H, s, $C(CH_3)_3$), 1.81−1.95 (1H, m, 2-CH_a), 2.15−2.32 (1H, m, 2-CH_b), 2.52 (1H, dd, J = 2.6 and 4.7 Hz, CH_aO), 2.78 (1H, t, J = 4.3 Hz, CH_bO), 2.98−3.07 (1H, m, CHO), 3.19 (2H, t, J = 8.0 Hz, 1-CH_2), 3.83 (2H, s, $SO_3CH_2C(CH_3)_3$); ^{13}C NMR (50 MHz) δ 25.99, 26.83, 31.72, 46.56, 47.20, 49.86, 78.86.

(±)-Neopentyl 2-Hydroxymethyl-cyclopropanesulfonate (31). A solution of (±)-**30** (0.45 g, 2.03 mmol) in dry THF (25 mL) was added to a stirred solution of 1 M LiHMDS in THF (4.66 mL, 4.6 mmol) kept at −30 °C in an argon atmosphere. After 3 h, the reaction mixture was allowed to warm to room temperature and then quenched with aqueous NH_4Cl (20 mL). The reaction mixture was extracted with EtOAc (5 × 50 mL). The combined organic phases were dried (Na_2SO_4), and the solvent was removed in vacuo to obtain a residue that was submitted to flash chromatography. Elution with light petroleum−EtOAc (8:2) afforded (±)-**31** (0.29 g, 65%). ^{1}H NMR (200 MHz) δ 0.96 (9H, s, $C(CH_3)_3$), 1.04−1.19 (1H, m, 1H, 3-CH_a), 1.35−1.48 (1H, m, 3-CH_b), 1.81−1.98 (1H, m, 2-CH), 2.38−2.46 (1H, m, 1-CH), 3.53 (1H, dd, J = 5.8 and 11.4 Hz, CH_aOH), 3.75 (1H, dd, J = 5.1 and 11.4 Hz, CH_bOH), 3.85 (2H, s, $SO_3CH_2C(CH_3)_3$); ^{13}C NMR (50 MHz) δ 9.48, 20.97, 25.99, 30.93, 31.73, 61.79, 79.48

(±)-Neopentyl 2-Formylcyclopropanesulfonate (26). A solution of (±)-**31** (0.86 g, 3.80 mmol) in dry CH_2Cl_2 (27 mL) was added dropwise to a stirred suspension of PCC (0.83 g, 3.80 mmol) in dry CH_2Cl_2 (27 mL) kept at room temperature, and the resulting mixture was stirred in an argon atmosphere for 3 h. The reaction mixture was then diluted with Et_2O (50 mL) and filtered, and the solvent was removed in vacuo to give a residue that was filtered through a Florisil pad to give (±)-**26** (0.57 g, 68%).

X-Ray Crystal Structure Determinations. Data collections have been carried out by using a Siemens *P*4 four-circle diffractometer with graphite monochromated Mo−Kα radiation (λ = 0.710 73 Å). The structures were solved by the direct methods implemented in the SHELXS-97 program.[57] The asymmetric unit of both *R*-SCG-3 (**13**) and *S*-SCG-3 (**12**) is formed by two crystallographic independent molecules and by one molecule in the case of *R*-SCG-1 (**10**). Structure refinements were carried out by full-matrix anisotropic

least-squares on F^2 for all reflections for all non-H atoms by using the SHELXL-97 program.[58] The hydrogen atoms were located on Fourier difference maps and were included in the structure-factor calculations, in some cases as riding atoms. The absolute configurations have been determined by the refined Flack parameter.[59] Molecular graphics were performed by using WinGX package.[60] Full crystal data and geometrical parameters of the crystal structures of *R*-SCG-3 (**12**), *S*-SCG-3 (**13**), and *R*-SCG-1 (**10**) are given as Supporting Information.

Molecular Modeling. The diversity space occupied by SCGs (**8**−**15**), CCGs (Chart 1), and PCGs (Chart 2) was calculated using the following computational protocol. All compounds were constructed starting from fragment dictionary and geometry optimized using the UNIVERSAL force field[61] with the Smart Minimizer protocol of Open Force Field (OFF). Atomic charges were computed using Gasteiger method. For each compound of both classes a set of 40 molecular descriptors was calculated. These descriptors included charged partial surface area descriptors (30) and shadow indices descriptors (10). These descriptors were calculated using Cerius-2. Charged partial surface area descriptors[62] capture shape and electronic information of molecules. They are calculated by mapping atomic partial charges on solvent-accessible surface areas of individual atoms. The surface indices are geometric descriptors that help to characterize the shape of the molecules. In particular, these descriptors are calculated by projecting the molecular surface on three mutually perpendicular planes, *XY*, *YZ*, and *XZ*.[63] Surface indices descriptors depend not only on conformation but also on the orientation of the molecule. To calculate them, the molecules are first rotated to align the principal moments of inertia with the *X*, *Y*, and *Z* axes. Then a consensus flexible alignment is performed with the Align module of Cerius2 using the common subgraph matching routine. The above descriptors were used as variables to perform a principal component analysis (PCA). The PCA was carried out using Cerius-2.

Docking experiments were performed using Autodock v3.0 into the crystal structures of GluR2-AMPA (pdb code 1ftj) and NR2A-NMDA (pdb code 2a5s).[64] Briefly, six experiments of 300 docking runs were carried out using the genetic algorithm with a population size of 50 individuals and 2 500 000 energy evaluations. Other parameters were left to their respective default values. The search was conducted in a grid of 60 points per dimension and a step size of 0.375 centered on the coordinates of the Cα atom of glutamate as resulting in the binding conformation of the crystal structures of AMPA and NMDA receptor. Results were clustered and ranked in terms of binding energy and occurrence for a given docked conformation. This protocol was tested for its ability in reproducing the binding disposition of *L*-Glu (**1**) observed in its crystal complexes with GluR2-AMPA and NR2A-NMDA.

The electrostatic potential of the receptors was calculated using the Finite Difference Poisson−Boltzmann method as implemented in Delphi module of Insight II software package.[65] The Poisson−Boltzmann method takes into account different values of the dielectric constant for the interior and the surrounding of the receptor allowing for the shielding effects of the solvent without the need to treat solvent molecules explicitly. By default, a dielectric constant of 2 was used for the interior of the receptor while a value of 80 was used for the surrounding of the receptor. The ionic strength of the solvent was set to 0.145 M (value at physiological pH). To analyze the electrostatic potentials, a grid cage of 65 points per dimension was defined and centered on the receptors. The percent of the grid occupied by the greatest Cartesian dimension of the solute was set to 30. The resulting grid resolution (grid step) was 0.33 Å. The potential values at the grid boundary points were calculated using the Debye−Huckel approximation with the exterior dielectric. The linear solution of the Poisson−Boltzmann equation was calculated with an automatic number of iterations and an energy convergence criteria of 10^{-6}. The atomic charge dictionary of Charmm22 was employed for the receptor atoms while the charges of ligand atoms were calculated using the semiempirical method Mopac-AM1. Ligands were considered in their ionized forms, with −1 as the formal charge of *L*-CCG IV (**5**) and *S*-SCG-4 (**15**). Because all charged residues of receptors were fully exposed to the solvent at least in their open conformation, basic and acidic residues were considered in their ionized forms.

Biological Assays. Subtypes of mGluRs (mGluR1, mGluR2, mGluR4, and mGluR5) expressed in BHK cells were cultured as previously described.[66] [^{3}H]-Quisqualate binding to mGluR1 and mGluR5 membranes were performed according to Mutel et al.,[67] [^{3}H]-(2*S*)-2-amino-2-[(1*S*,2*S*)-2-carboxycycloprp-1-yl]-3-(xanth-9-yl)propanoic acid ([^{3}H]-LY341495) binding to mGluR2 and [^{3}H]-*L*-AP4 binding to mGluR4 were conducted as detailed previously.[68,69] Affinities for native AMPA, kainate, and NMDA receptors were determined using 5 nM [^{3}H]-AMPA, 5 nM [^{3}H]-kainic acid, and 2 nM [^{3}H]-*D*,*L*-(*E*)-2-amino-4-propyl-5-phosphono-3-pentenoic acid ([^{3}H]-CGP39653) as previously described.[70] In brief, frozen rat brain membranes were quickly thawed and homogenized in 40 volumes of ice-cold buffer (pH 7.4, 30 mM Tris−HCl containing 2.5 mM $CaCl_2$, 50 mM Tris−HCl or 50 mM Tris−HCl containing 2.5 mM $CaCl_2$, for [^{3}H]-AMPA, [^{3}H]-kainic acid or [^{3}H]-CGP39653 binding, respectively) and centrifuged at 48 000 × *g* for 10 min. This procedure was repeated four times. In [^{3}H]-AMPA binding experiments, 100 mM KSCN was added to the buffer during the final wash and during incubation. The final pellet was resuspended in ice-cold buffer, corresponding to approximately 0.4−0.5 mg protein/mL. [^{3}H]-AMPA, [^{3}H]-kainic acid, and [^{3}H]-CGP39653 binding were carried out in aliquots consisting of radioligand (25 μL), test solution (25 μL), and membrane suspension (200 μL) and incubated for 30, 60, and 60 min, respectively. Binding was terminated by filtration through GF/B filters and washing with 3 × 250 μL buffer and bound radioactivity was counted on a Topcounter (Packard). Nonspecific binding was determined using 1 mM *L*-Glu.

Supporting Information Available: X-ray crystallographic data for compounds **10**, **12**, and **13**; elemental analyses for compounds **8**−**15**; and HPLC tracings for compounds **8**−**15** and **32**−**39**. This material is available free of charge via the Internet at http://pubs.acs.org.

References

(1) Pellicciari, R.; Curini, M.; Natalini, B.; Ceccherelli, P. *Abstract of the IX International Symposium on Medicinal Chemistry*, Berlin, Germany, 1986; p 118.
(2) Pellicciari, R.; Natalini, B.; Monahan, J. B.; Lanthorn, T. H.; Pilipauskas, D.; Snyder, J. P. *6th Camerino-Noordwijkerout Symposium on Recent Advances in Receptor Chemistry*, Camerino, Italy, 1987; pp 73−74.
(3) Pellicciari, R.; Natalini, B.; Marinozzi, M., et al. In *Frontiers in Excitatory Amino Acid Research*; Cavalheiro, E. A., Lehman, J., Turski. L., Eds.; Alan R. Liss, Inc.: New York, 1988; p 67.
(4) Shinozaki, H.; Ishida, M.; Shimamoto, K.; Ohfune, Y. Potent NMDA-like actions and potentiation of glutamate responses by conformational variants of a glutamate analogue in the rat spinal cord. *Br. J. Pharmacol.* **1989**, *98*, 1213−1224.
(5) Kawai, M.; Horikawa, Y.; Ishihara, T.; Shimamoto, K.; Ohfune, Y. 2-(Carboxycyclopropyl)glycines: binding, neurotoxicity and induction of intracellular free Ca^{2+} increase. *Eur. J. Pharmacol.* **1992**, *211*, 195−202.
(6) Ishida, M.; Akagi, H.; Shimamoto, K.; Ohfune, Y.; Shinozaki, H. A potent metabotropic glutamate receptor agonist: electrophysiological actions of a conformationally restricted glutamate analogue in the rat spinal cord and Xenopus oocytes. *Brain Res.* **1990**, *537*, 311−314.
(7) Amori, L.; Serpi, M.; Marinozzi, M.; Costantino, G.; Gavilan Diaz, M.; Hermit, M. B.; Thomsen, C.; Pellicciari, R. Synthesis and preliminary biological evaluation of (2*S*,1′*R*,2′*S*)- and (2*S*,1′*S*,2′*R*)-2-(2-phosphonocyclopropyl)glycines, two novel conformationally constrained *L*-AP4 analogues. *Bioorg. Med. Chem. Lett.* **2006**, *16*, 196−199.
(8) Macchiarulo, A.; Pellicciari, R. Exploring the other side of biologically relevant chemical space: Insights into carboxylic, sulfonic and phosphonic bioisosteric relationships. *J. Mol. Graph. Model.* **2007**, doi:10.1016/j.jmgm.2007.04/010.
(9) Griffiths, R. The biochemistry and pharmacology of excitatory sulphur-containing amino acids. *Biochem. Soc. Trans.* **1993**, *21*, 66−72.

(10) Grandes, P.; Morino, P.; Cuenod, M.; Streit, P. Homocysteate, an excitatory transmitter candidate localized in glia. *Eur. J. Neurosci.* **1991**, *3*, 1370−1373.

(11) Grieve, A.; Griffiths, R. Simultaneous measurement by HPLC of the excitatory amino acid transmitter candidates homocysteate and homocysteine sulphinate supports a predominant astrocytic localisation. *Neurosci. Lett.* **1992**, *145*, 1−5.

(12) Zhang, N.; Ottersen, O. P. Differential cellular distribution of two sulphur-containing amino acids in rat cerebellum. An immunocytochemical investigation using antisera to taurine and homocysteic acid. *Exp. Brain Res.* **1992**, *90*, 11−20.

(13) Azkue, J.; Mateos, J. M.; Cuenod, M.; Streit, P.; Grandes, P. Immunohistochemical localization of homocysteate in human primary visual cortex. *NeuroReport* **1995**, *7*, 318−320.

(14) Do, K. Q.; Benz, B.; Sorg, O.; Pellerin, L.; Magistretti, P. J. beta-Adrenergic stimulation promotes homocysteic acid release from astrocyte cultures: Evidence for a role of astrocytes in the modulation of synaptic transmission. *J. Neurochem.* **1997**, *68*, 2386−2394.

(15) Benz, B.; Grima, G.; Do, K. Q. Glutamate-induced homocysteic acid release from astrocytes: Possible implication in glia-neuron signaling. *Neuroscience* **2004**, *124*, 377−386.

(16) Freeman, M. R. Sculpting the nervous system: glial control of neuronal development. *Curr. Opin. Neurobiol.* **2006**, *16*, 119−125.

(17) Haydon, P. G. GLIA: Listening and talking to the synapse. *Nat. Rev. Neurosci.* **2001**, *2*, 185−193.

(18) Do, K. Q.; Benz, B.; Binns, K. E.; Eaton, S. A.; Salt, T. E. Release of homocysteic acid from rat thalamus following stimulation of somatosensory afferents in vivo: Feasibility of glial participation in synaptic transmission. *Neuroscience* **2004**, *124*, 387−393.

(19) Gortz, P.; Hoinkes, A.; Fleischer, W.; et al. Implications for hyperhomocysteinemia: Not homocysteine but its oxidized forms strongly inhibit neuronal network activity. *J. Neurol. Sci.* **2004**, *218*, 109−114.

(20) Levine, J.; Stahl, Z.; Sela, B. A.; Ruderman, V.; Shumaico, O.; Babushkin, I.; Osher, Y.; Bersudsky, Y.; Belmaker, R. H. Homocysteine-reducing strategies improve symptoms in chronic schizophrenic patients with hyperhomocysteinemia. *Biol. Psychiatry* **2006**, *60*, 265−269.

(21) Miller, J. W. Homocysteine, Alzheimer's disease, and cognitive function. *Nutrition* **2000**, *16*, 675−677.

(22) Levine, J.; Stahl, Z.; Sela, B. A.; Gavendo, S.; Ruderman, V.; Belmaker, R. H. Elevated homocysteine levels in young male patients with schizophrenia. *Am. J. Psychiatry* **2002**, *159*, 1790−1792.

(23) Morris, M. S.; Jacques, P. F.; Rosenberg, I. H.; Selhub, J. Hyperhomocysteinemia associated with poor recall in the third National Health and Nutrition Examination Survey. *Am. J. Clin. Nutr.* **2001**, *73*, 927−933.

(24) van der Put, N. M.; van Straaten, H. W.; Trijbels, F. J.; Blom, H. J. Folate, homocysteine and neural tube defects: An overview. *Exp. Biol. Med.* **2001**, *226*, 243−270.

(25) (a) Zimmermann, H. E.; Thyagarajan, B. S. The stereochemistry of sulfone-stabilized carbanions. *J. Am. Chem. Soc*. **1960**, *82*, 2505−2511. (b) Truce, W. E.; Lindy, L. B. Cyclopropyl sulfones. *J. Org. Chem.* **1961**, *26*, 1463−1467.

(26) Truce, W. E.; Goralski, C. T. *trans*-1-(Arenesulfonyl)-2-arylcyclopropanes and derivatives of cyclopropanesulfonic acid. *J. Org. Chem.* **1969**, *34*, 3324−3328.

(27) Truce, W. E.; Goralski, C. T. Cyclopropanesulfonic acid esters and amides. *J. Org. Chem*. **1968**, *33*, 3849−3851.

(28) Zindel, J.; de Meijere, A. A short and efficient diastereoselective synthesis of 2′-substituted 2-cyclopropylglycines. *Synthesis* **1994**, 190−194.

(29) Strating, J.; van Leusen, A. M. Chemistry of α-diazosulphones. Part I. Preliminary communication. *Rec. Trav. Chim.* **1962**, *81*, 966−968.

(30) (a) van Leusen, A. M.; Strating, J. Chemistry of α-diazosulphones. Part V. The synthesis of arylsulfonyldiazomethanes and alkylsulfonyldiazomethanes. *Rec. Trav. Chim*. **1965**, *84*, 151−164. (b) van Leusen, A. M.; Strating, J. *p*-Tolylsulfonyldiazomethane. *Org. Synth*. **1977**, *57*, 85−102.

(31) Regitz, M. Recent synthetic methods in diazo chemistry. *Synthesis* **1972**, 351−373 and references cited therein.

(32) van Leusen, A. M.; Strating, J.; van Leusen, D. On the synthesis of α-phenyltosyldiazomethane. *Tetrahedron Lett.* **1973**, 5207−5208.

(33) Hua, D. H.; Peacock, N. J.; Meyers, C. Y. Synthesis of a sulfone α-tosylate. Benzyl(tosyloxy)methyl sullfone. *J. Org. Chem*. **1980**, *45*, 1717−1719.

(34) van Leusen, A. M.; Mulder, R. J.; Strating, J. Chemistry of α-diazosulphones. A sulphonylcarbene. *Tetrahedron Lett.* **1964**, 543−546.

(35) (a) Padwa, A.; Wannamaker, M. W.; Dyszlewski, A. D. Chemical reactivity and configurational properties of cyclopropyl carbanions derived from a silyl sulfonyl substituted cyclopropene. *J. Org. Chem.* **1987**, *52*, 4760−4767. For examples on α-diazo-*β*-keto sulfones, see: (b) Honma, M.; Sawada, T.; Fujisawa, Y.; Utsugi, M.; Watanabe, H.; Umino, A.; Matsumura, T.; Hagihara, T.; Takano, M.; Nakada, M. Asymmetric catalysis on the intramolecular cyclopropanation of α-diazo-*β*-keto sulfones. *J. Am. Chem. Soc*. **2003**, *125*, 2860−2861. (c) Kennedy, M.; McKervey, A.; Maguire, A. R.; Roos, H. P. Asymmetric synthesis in carbon-carbon bond forming reactions of α-diazoketones catalysed by homochiral rhodium (II)carboxylates. *J. Chem. Soc., Chem Commun.* **1990**, 361.

(36) Berkessel, A.; Voges, M. 1-Formyl-1-diazoalkanesulfonates. *Chem. Ber*. **1989**, *122*, 1147−1151.

(37) Ye, T.; Zhou, C. Enantiocontrol in intermolecular cyclopropanations: Use of diazosulfonate. *New J. Chem*. **2005**, *29*, 1159−1163.

(38) (a) Truce, W. E.; Norell, J. R. Reactions of 3,3-diethoxythietane 1,1-dioxide and 2-phenyl-3,3-diethoxythietane 1,1-dioxide. *J. Am. Chem. Soc.* **1963**, *85*, 3231−3236. (b) Truce, W. E.; Vrencur, D. J. α-Alkylation of alkyl alkanesulfonates. *J. Org. Chem*. **1970**, *35*, 1226−1227.

(39) Chakraborty, T. K.; Hussian, K. A.; Reddy, G. V. α-Phenylglycinol as chiral auxiliary in diastereoselective Strecker synthesis of α-amino acids. *Tetrahedron* **1995**, *51*, 9179−9190.

(40) Pellicciari, R.; Marinozzi, M.; Natalini, B.; Costantino, G.; Luneia, R.; Giorgi, G.; Moroni, F.; Thomsen, C. Synthesis and pharmacological characterization of all sixteen stereoisomers of 2-(2′-carboxy-3′-phenylcyclopropyl)glycine. Focus on (2*S*,1′*S*,2′*S*,3′*R*)-2-(2′-carboxy-3′-phenylcyclopropyl) glycine, a novel and selective group II metabotropic glutamate receptors antagonist. *J. Med. Chem*. **1996**, *39*, 2259−2269.

(41) Watkins, J. C.; Evans, R. H. Excitatory amino acid transmitters. *Annu. Rev. Pharmacol. Toxicol.* **1981**, *21*, 165−204.

(42) Mayer, M. L.; Westbrook, G. L. Mixed-agonist action of excitatory amino acids on mouse spinal cord neurones under voltage clamp. *J. Physiol.* **1984**, *354*, 29−53.

(43) Pullan, L. M.; Olney, J. W.; Price, M. T.; et al. Excitatory amino acid receptor potency and subclass specificity of sulfur-containing amino acids. *J. Neurochem.* **1987**, *49*, 1301−1307.

(44) Porter, R. H.; Roberts, P. J. Glutamate metabotropic receptor activation in neonatal rat cerebral cortex by sulphur-containing excitatory amino acids. *Neurosci. Lett.* **1993**, *154*, 78−80.

(45) Yuzaki, M.; Connor, J. A. Characterization of *L*-homocysteate-induced currents in Purkinje cells from wild-type and NMDA receptor knockout mice. *J. Neurophysiol.* **1999**, *82*, 2820−2826.

(46) Shi, Q.; Savage, J. E.; Hufeisen, S. J.; et al. *L*-Homocysteine sulfinic acid and other acidic homocysteine derivatives are potent and selective metabotropic glutamate receptor agonists. *J. Pharmacol. Exp. Ther*. **2003**, *305*, 131−142.

(47) Wermuth, C. G. *The practice of medicinal chemistry*; Academic Press: New York, 1996.

(48) Tintelnot, M.; Andrews, P. Geometries of functional group interactions in enzyme-ligand complexes: Guides for receptor modelling. *J. Comput.-Aided Mol. Des*. **1989**, *3*, 67−84.

(49) Klebe, G. The use of composite crystal-field environments in molecular recognition and the de novo design of protein ligands. *J. Mol. Biol*. **1994**, *237*, 212−235.

(50) Roe, S. M.; Teeter, M. M. Patterns for prediction of hydration around polar residues in proteins. *J. Mol. Biol.* **1993**, *229*, 419−427.

(51) Kanyo, Z. F.; Christianson, D. W. Biological recognition of phosphate and sulfate. *J. Biol. Chem*. **1991**, *266*, 4264−4268.

(52) Pirard, B.; Baudoux, G.; Durant, F. A database study of intermolecular NH−O hydrogen bonds for carboxylates, sulfonates and monohydrogen phosphonates. *Acta Crystallogr., Sect. B: Struct. Sci*. **1995**, *B51*, 103−107.

(53) Costantino, G.; Natalini, B.; Pellicciari, R.; Lombardi, G.; Moroni, F. Definition of a pharmacophore for metabotropic glutamte receptors negatively linked to adenylyl cyclase. *Bioorg. Med. Chem*. **1993**, *1*, 259−265.

(54) Costantino, G.; Macchiarulo, A.; Pellicciari, R. Pharmacophore models of group I and group II metabotropic glutamate receptor agonists. Analysis of conformational, steric, and topological parameters affecting potency and selectivity. *J. Med. Chem*. **1999**, *42*, 2816−2827.

(55) Armstrong, N.; Gouaux, E. Mechanisms for activation and antagonism of an AMPA-sensitive glutamate receptor: Crystal structures of the GluR2 ligand binding core. *Neuron* **2000**, *28*, 165−181.

(56) Furukawa, H.; Singh, S. K.; Mancusso, R.; Gouaux, E. Subunit arrangement and function in NMDA receptors. *Nature* **2005**, *438*, 185−192.

(57) Sheldrick, G. M. *SHELXS-97*, Rel. 97-2, A program for automatic solution of crystal structures; Göttingen University: Göttingen, Germany, 1997.

(58) Sheldrick, G. M. *SHELXL-97*, Rel. 97-2, A program for crystal structure refinement; Göttingen University: Göttingen, Germany, 1997.

(59) Flack, H. D. On enantiomorph-polarity estimation. *Acta Crystallogr., Sect. A: Found. Crystallogr*. **1983**, *A39*, 876−881.
(60) Farrugia, L. J. WinGX suite for small molecule single crystal crystallography *J. Appl. Cryst.* **1999**, *32*, 837−838.
(61) Kappe, A. K.; Casewit, C. J.; Colwell, K. S.; Goddard, W. A.; Skiff, W. M. UFF, a full periodic table force field for molecular mechanics and molecular dynamics simulations. *J. Am. Chem. Soc*. **1992**, *114*, 10024−10035.
(62) Stanton, D. T.; Jurs, P. C. Development and use of charged partial surface area structural descriptors in computer-assisted quantitative structure-property relationship studies. *Anal. Chem*. **1990**, *62*, 2323−2329.
(63) Rohrbaugh, R. H.; Jurs, P. C. Descriptions of molecular shape applied in studies of structure/activity and structure/property relationships. *Anal. Chim. Acta* **1987**, *199*, 99−109.
(64) Morris, G. M.; Goodsell, D. S.; Halliday, R. S.; Huey, R.; Hart, W. E. Automated docking using lamarckian genetic algorithm and empirical binding free energy function. *J. Comput. Chem.* **1998**, *19*, 1639−1662.
(65) Klapper, I.; Hagstrom, R.; Fine, R.; Sharp, K.; Honig, B. Focusing of electric fields in the active site of Cu-Zn superoxide dismutase: Effects of ionic strength and amino-acid modification. *Proteins* **1986**, *1*, 47−59.
(66) Mathiesen, J. M.; Svendsen, N.; Brauner-Osborne, H.; Thomsen, C.; Ramirez, M. T. Positive allosteric modulation of the human metabotropic glutamate receptor 4 (hmGluR4) by SIB-1893 and MPEP. *Br. J. Pharmacol*. **2003**, *138*, 1026−1030.
(67) Mutel, V.; Ellis, G. J.; Adam, G.; Chaboz, S.; Nilly, A.; Messer, J.; Bleuel, Z.; Metzier, V.; Malherbe, P.; Achlaeger, E. J.; Roughley, B. S.; Faull, R. L.; Richards, J. G. Characterization of [^{3}H]-quisqualate binding to recombinant rat metabotropic glutamate 1a and 5a receptors and to rat and human brain sections. *J. Neurochem*. **2000**, *75*, 2590−2601.
(68) Johnson, B. G.; Wright, R. A.; Arnold, M. B.; Wheeler, W. J.; Ornstein, P. L.; Schoepp, D. D. [^{3}H]-LY341495 as a novel antagonist radioligand for group II metabotropic gluatmate (mGlu) receptors: characterization of binding to membranes of mGlu receptor subtype expressing cells. *Neuropharmacology* **1999**, *38*, 1519−1529.
(69) Eriksen, L.; Thomsen, C. [^{3}H]-L-2-Amino-4-phosphonobutyrate labels a metabotropic glutamate receptor, mGluR4a. *Br. J. Pharmacol.* **1995**, *116*, 3279−3287.
(70) Hermit, M. B.; Grenwood, J. R.; Nielsen, B.; Bunch, L.; Jorgensen, C. G.; Vestergaard, H. T.; Stenbol, T. B.; Sanchez, C.; Krogsgaard-Larsen, P.; Madsen, U.; Brauner-Osborne, H. Ibotenic acid and thioibotenic acid: A remarkable difference in the activity at group III metabotropic glutamate receptors. *Eur. J. Pharmacol*. **2004**, *486*, 241−250.

JM070322E